arXiv:1703.02280v1 [cond-mat.mes-hall] 7 Mar 2017

Weak Measurement of Quantum Superposition States in Graphene

Maxim Trushin, Johannes Bülte, and Wolfgang Belzig
University of Konstanz, Fachbereich Physik, M703 D-78457 Konstanz
(Dated: March 8, 2017)

We employ a weak measurement approach to demonstrate the very existence of the photoexcited interband superposition states in intrinsic graphene. We propose an optical two-beam setup where such measurements are possible and derive an explicit formula for the differential optical absorption that contains a signature of such states. We provide an interpretation of our results in terms of a non-Markovian weak measurement formalism applied to the pseudospin degree of freedom coupled with an electromagnetic wave.

Introduction. — Quantum coherence is among the most subtle concepts in quantum mechanics: It cannot be directly observed because any superposition state collapses immediately to an eigenstate of the operator corresponding to the observable one is trying to measure[1]. In attempts to circumvent the projection postulate, the concept of weak measurements has been introduced nearly 30 years ago[2]. To perform a weak measurement[3] of a quantum state ψ the detector must also represent a quantum mechanical object described by a wave function ψ'. The measured system interacts with the detector, and it is the detector's wave function ψ' that is collapsed by a strong measurement. Due to the interaction between these two states the outcome of the measurement on ψ' contains some information about coherence of the original quantum state ψ. In the past decade several experimental attempts have been made to measure coherent superpositions with photons[4–8] and, more recently, with nuclear spins[9,10]. Despite theoretical efforts[11–13] the interpretation of weak measurements remains controversial[14,15].

In this Letter, we shift the focus of this problem to photocarriers in semiconductors, namely, we propose an experiment to measure the photoexcited interband (pseudospin) superposition states in intrinsic graphene. Our quantum steady state is created by linearly polarized monochromatic radiation and described by a 2×2 photocarrier density matrix f_{ij} including non-zero coherences representing interband superpositions, see Fig. 1. The probe radiation in turn creates a density matrix f'_{ij} that depends on f_{ij} but is collapsed by a strong measurement of the photocarrier occupation. We show that the differential relative absorption of the probe radiation, see Fig. 2, contains a certain quantum information about initial superposition states encoded in f_{ij}.

Model in depth. — The effective two-level system shown in Fig. 1 is described by the two-dimensional massless Dirac-like Hamiltonian[16] $\hat{H}_0 = \hbar v \hat{\sigma}\cdot\hat{\mathbf{k}}$, where $\hbar\hat{\mathbf{k}}$ is the two-component momentum operator, $\hat{\sigma}$ is the pseudospin operator constructed from the Pauli matrices, and $v \approx 10^6$ ms^{-1} is the carrier velocity in graphene. The corresponding eigenvalues and eigenstates are $E_{1,2} = \pm\hbar v k$ and $\psi_{1,2} = \frac{1}{\sqrt{2}}(1, \pm e^{i\phi})$ with $\tan\phi = k_y/k_x$. The index 1 (2) stands for the conduction (valence) band respectively, see Fig. 1. The pseudospin is parallel (antiparallel) to momentum while being in a conduction (valence) band eigenstate. Hence, a certain interband coherent state $\psi = a\psi_1 + b\psi_2$ we are trying to measure represents, at the same time, a pseudospin superposition state.

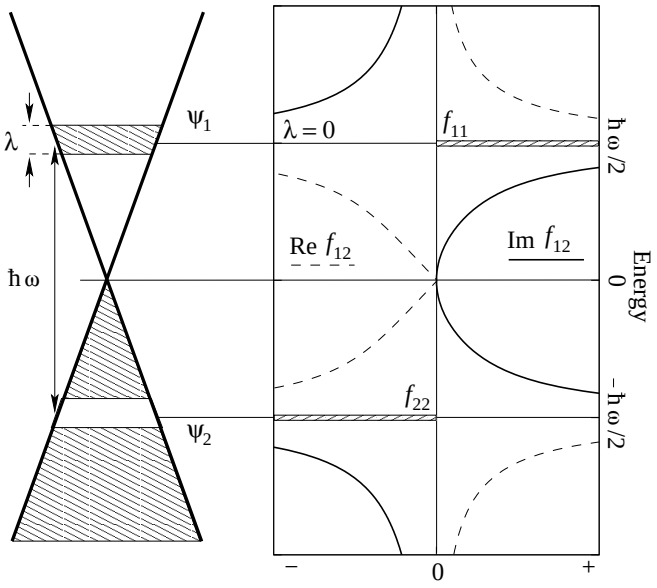

FIG. 1. Direct interband excitations result not only in the photocarrier occupations f_{11}, $f_{22} = -f_{11}$ at energies $\pm\hbar\omega/2$, but also in the coherences f_{12}, $f_{21} = f_{12}^*$ representing the superpositions between conduction and valence band eigenstates. The matrix f_{ij} can be seen as a density matrix written in the eigenstate basis of $\hat{H}_0$. In the right diagram the density matrix components are shown in arbitrary units assuming perfectly monochromatic radiation ($\lambda = 0$, i.e. f_{ii} shrinks to a δ-function). Note that Ref_{12} vanishes faster than Imf_{12} when the energy increases, i.e. the latter dominates in the high energy tail of the density matrix representing the signature of the quantum superposition states.

In order to create and measure such a superposition state we employ an electromagnetic wave $\mathcal{E}(t) = \mathcal{E}_0\left(e^{i\omega t} + e^{-i\omega t}\right)\hat{\mathbf{e}}$ with the frequency ω and amplitude $\mathcal{E}_0$ linearly-polarized in the direction $\hat{\mathbf{e}}$. The equilibrium carriers are then perturbed by the field-pseudospin interaction[17] $\hat{H}_{\rm int}(t) = \hat{h}\left(e^{i\omega t} + e^{-i\omega t}\right)$, where $\hat{h} = \frac{ev\mathcal{E}_0}{2\omega}\hat{\sigma}\cdot\hat{\mathbf{e}}$ with e being the electron charge. We assume normal incidence without momentum transfer from photons to electrons so that we always superimpose the states $\psi_{1,2}$

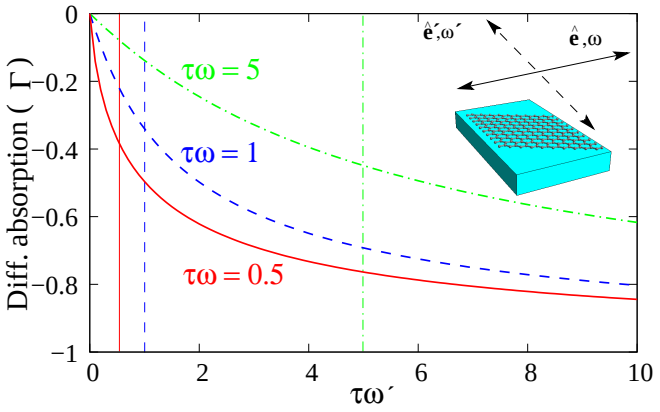

FIG. 2. Graphene is irradiated by two CW monochromatic light beams having the frequencies ω and ω' and linear polarizations perpendicular to each other. One of the beams creates an initial photocarrier distribution, whereas another is used as a weak measurement probe. The curves represent relative optical absorption difference *vs.* detector's excitation frequency ω' in units of $1/\tau$ (dephasing rate) at zero temperature and zero doping, as given by Eq. (11). The differential relative absorption is given in units of Γ, see Eq. (12). The verticals show the initial photocarrier occupation positions that have shrunk to zero due to the perfectly monochromatic radiation.

with the same momentum. It is convenient to define the coupling parameter $\eta_\omega = \frac{ev\mathcal{E}_0}{2\omega}$ that entangles the electric field and the pseudospin $\hat{\sigma}$. In contrast to conventional semiconductors, where a similar coupling constant can also be defined, graphene allows tuning η_ω in a very broad range and in a very predictable manner. Indeed, the excitation frequency ω can be shifted from the ultraviolet to far infrared regions while keeping the photocarrier velocity constant, hence, changing η_ω by orders of magnitude. In conventional semiconductors the lowest possible ω is limited by the band gap, and the photocarrier velocity is dependent on the excitation frequency reflecting their complicated band structure. Thus, graphene offers an unprecedented opportunity to study the pseudospin (or interband) coherence by optical means.

Creating a pseudospin superposition state. — The operator $\hat{h}$ written in the eigenbasis of $\hat{H}_0$ is given by the matrix

$$\hat{h} = \eta_\omega \begin{pmatrix} \cos(\phi-\theta) & -i\sin(\phi-\theta) \\ i\sin(\phi-\theta) & -\cos(\phi-\theta) \end{pmatrix}, \qquad (1)$$

where $\tan\theta = e_y/e_x$ describes the polarization plane orientation. The pseudospin-momentum coupling in graphene results in both off- and diagonal terms in Eq. (1) responsible for the generation of coherences in the electron density matrix. This is the crucial ingredient that makes the optical generation and detection of superposition states possible. It is natural to describe the pseudospin coherence by a 2×2 density matrix $\hat{\rho}$ whose evolution is governed by the Liouville-von Neumann equation $\partial_t\hat{\rho} + \frac{i}{\hbar}[\hat{H}_0, \hat{\rho}(t)] = \hat{g}(t)$, where the generation rate is given in the lowest non-zero order in h by[18]

$$\hat{g}(t) = -\frac{1}{\hbar^2}\int\limits_{-\infty}^{0} dt' \mathrm{e}^{\lambda t'} \left\{ \left(\mathrm{e}^{i\omega t'} + \mathrm{e}^{-i\omega t'} \right) \times [\hat{h}, \mathrm{e}^{\frac{i}{\hbar}\hat{H}_0 t'}[\hat{h}, \hat{\rho}(t+t')]\mathrm{e}^{-\frac{i}{\hbar}\hat{H}_0 t'}] \right\}. \qquad (2)$$

Here, the adiabaticity parameter $\lambda > 0$ has been introduced in order to take into account the finite Lorentzian spectral width of the radiation flow. We assume that $\lambda \to 0$ at the end of the day. This approximation corresponds to the continuous wave (CW) operation of the laser. We now write the density matrix $\hat{\rho}$ and the corresponding Liouville-von Neumann equation in the eigenstate basis of $\hat{H}_0$ (helicity basis), and, at the same time, add relaxation and dephasing terms. The equation then reads

$$\frac{\partial}{\partial t}\begin{pmatrix} f_{11} & f_{12} \\ f_{21} & f_{22} \end{pmatrix} + \frac{i}{\hbar}\begin{pmatrix} 0 & f_{12}(E_1-E_2) \\ f_{21}(E_2-E_1) & 0 \end{pmatrix} = \begin{pmatrix} g_{11}[f^0] & g_{12}[f^0] \\ g_{21}[f^0] & g_{22}[f^0] \end{pmatrix} - \begin{pmatrix} f_{11}/\tau_0 & f_{12}/\tau \\ f_{21}/\tau & f_{22}/\tau_0 \end{pmatrix}, \qquad (3)$$

where the functions f_{ij} represent the change in the density matrix $\hat{\rho} - \hat{\rho}^{\mathrm{eq}}$ written in basis of the unperturbed eigenstates of $\hat{H}_0$, f^0 is the equilibrium distribution matrix diagonal in the same basis, τ_0 is the relaxation time, τ is the dephasing time. The generation rate is transformed within the rotating wave approximation[19] and reads

$$g_{11}[f^0] = \frac{2h_{12}h_{21}}{\hbar^2}\left(f_{22}^{(0)} - f_{11}^{(0)}\right) \times \sum_{\pm}\frac{\lambda}{\lambda^2 + (\Omega \pm \omega)^2}, \qquad (4)$$

$$g_{12}[f^0] = \frac{h_{11}h_{12} + h_{21}h_{22}}{\hbar^2}\left(f_{11}^{(0)} - f_{22}^{(0)}\right) \times \sum_{\pm}\frac{1}{\lambda + i(\Omega \pm \omega)}, \qquad (5)$$

and $g_{22} = -g_{11}$, $g_{21} = g_{12}^*$. Here, $\Omega = (E_1 - E_2)/\hbar = 2vk$. Note that g_{11} is proportional to a δ-function at $\lambda \to 0$, whereas g_{12} is not. Since the interaction matrix h_{ij} contains *both* diagonal and non-diagonal terms, the generation rate g_{ij} does the same. This is the reason why the light-carrier interaction creates the interband coherent states. If the generation g_{ij} were turned off at $t = 0$, then the coherences in f_{ij} would be given by $f_{12}(t) = f_{12}(0)\exp(-t/\tau - i\Omega t)$, $f_{21} = f_{12}^*$ representing a rapidly oscillating function with the amplitude determined by the initial condition at $t = 0$. Measuring such an oscillating function could be a challenging task and, therefore, we focus on a steady-state limit, when $\partial f_{ij}/\partial t = 0$. In this limit, the solution of (3) is given by $f_{12} = \tau g_{12}[f^0]/(1 + i\tau\Omega)$, $f_{11} = \tau_0 g_{11}[f^0]$, $f_{21} = f_{12}^*$, $f_{22} = -f_{11}$. At $\lambda \to 0$, the diagonal terms f_{ii} represent occupations of the corresponding bands given by the

delta function $\delta(\Omega-\omega)$ whereas the coherences f_{ij} describe the pseudospin superposition states and remain finite even at $\Omega\neq\omega$.

Measuring the superposition state. — The interband coherences schematically depicted in Fig. 1 are generated by $\hat{H}_{\rm int}$ which couples the electric field and pseudospin — the quantity we are trying to measure. The weak measurement is performed by means of the interaction between the probe electromagnetic wave and pseudospin: $\hat{H}'_{\rm int}=\hat{h}'\left(\mathrm{e}^{i\omega' t}+\mathrm{e}^{-i\omega' t}\right)$ with $\hat{h}'=\frac{ev\mathcal{E}'_0}{2\omega'}\hat{\sigma}\cdot\hat{\mathbf{e}}'$, where $\hat{\mathbf{e}}'\perp\hat{\mathbf{e}}$. The orthogonality between $\hat{\mathbf{e}}'$ and $\hat{\mathbf{e}}$ allows us to filter out the absorption of any of these two electromagnetic waves easily. Similar to $\hat{h}$, the electric field amplitude $\mathcal{E}'_0$ and pseudospin $\hat{\sigma}$ are coupled by the coupling parameter $\eta_{\omega'}=\frac{ev\mathcal{E}'_0}{2\omega'}$. The probe radiation is assumed to have the intensity $I'_0=c{\mathcal{E}'}_0^2/8\pi$ much lower than $I_0=c\mathcal{E}_0^2/8\pi$ so that the probe almost does not change the coherent state created initially by $\hat{h}$. It is also crucial for the probe interaction $\hat{h}'$ to be weak enough to justify the weak measurement criterion within the whole frequency interval we are interested in, i.e. the probe intensity should be tuned while changing the probe frequency ω' so that $\eta_{\omega'}$ remains constant. The complete quantum mechanical weak measurement procedure also requires averaging over many single weak measurements[3]. Since we employ the density matrix (not a wave function) for the quantum state description, the statistics is taken into account automatically within our model. In the experiment, the CW operating probe serves for the desired statistics.

The probe generation rate $\hat{g}'(t)$ is formally given by the equation similar to Eq. (2), but the resulting $g'_{ij}[f]$ depends not only on the band occupations f_{11}, f_{22} but also on the coherences f_{12}, f_{21} introduced above. The coherences vanish in equilibrium, however, once the steady-state non-equilibrium is created, the coherences can be observed by measuring the optical absorption calculated from $g'_{ij}[f]$. The relative optical absorption is defined as $A=I'/I'_0$, where I' is the absorbed intensity per spin/valley channel given by $I'=\hbar\omega'\int d^2k g'_{11}/(2\pi)^2$. Here, we need only one component of the generation matrix g'_{ij} representing the valence-to-conduction band transition rate given by

$$g'_{11}[f]=\sum_{\pm}\frac{h'_{12}h'_{21}}{\hbar^2}\frac{2\lambda\left(f_{22}-f_{11}\right)}{\lambda^2+(\Omega\pm\omega')^2} \qquad (6)$$
$$-2i\sum_{\pm}\frac{h'_{12}h'_{22}}{\hbar^2}\frac{(\Omega\pm\omega')\mathrm{Re}f_{12}-\lambda\mathrm{Im}f_{12}}{\lambda^2+(\Omega\pm\omega')^2}.$$

The first term formally looks similar to Eq. (4) but the equilibrium occupations f^0_{ii} are substituted by their steady-state counterparts f_{ii} determined by the relaxation time τ_0. This term dominates in the absorption at $\omega=\omega'$ and corresponds to the conventional signal in the optical pump-probe measurements[20]. The second term contains quantum information about the initial steady-state via coherences f_{ij} determined by the dephasing time τ. At $\lambda\to 0$, $\mathrm{Im}f_{12}$ and $\mathrm{Re}f_{12}$ are weighted in the relative absorption by the delta-function $\delta(\Omega\pm\omega')$ and the principle value $1/(\Omega\pm\omega')$ respectively. $\mathrm{Im}f_{12}$ dominates in the absorption at $\omega'>>\omega$.

The description in terms of a non-Markovian weak measurement formalism[21] can provide insight into the interaction of the probe beam and the pseudospin. Starting from a microscopic model, the field-field correlator of the outgoing electric field after the interaction with the graphene is given by

$$\langle\mathcal{E}'(0)\mathcal{E}'(0)\rangle_w \qquad (7)$$
$$=\frac{1}{2\hbar^2}\int dt\int dt'\chi(0,t)\chi(0,t')\langle\{\hat{\sigma}_x(t),\hat{\sigma}_x(t')\}\rangle$$
$$-\frac{2i}{\hbar^2}\int dt\int dt'\theta(t-t')\chi(0,t)S(0,t')\langle[\hat{\sigma}_x(t),\hat{\sigma}_x(t')]\rangle,$$

where $\chi(0,t)=-i\frac{\eta_{\omega'}}{\sqrt{N}}\theta(-t)\mathrm{e}^{\lambda t}\langle[\hat{\mathcal{E}}'(0),\hat{\mathcal{E}}'(t)]\rangle$ is the response function and $S(0,t)=\frac{\eta_{\omega'}}{2\sqrt{N}}\mathrm{e}^{\lambda|t|}\langle\{\hat{\mathcal{E}}'(0),\hat{\mathcal{E}}'(t)\}\rangle$ is the noise function of the probe beam. Note, that the dimensionless electric field $\hat{\mathcal{E}}'=\frac{i}{\sqrt{2}}(\hat{a}\mathrm{e}^{-i\omega' t}-\hat{a}^\dagger\mathrm{e}^{i\omega' t})$ is quantized in this formalism and the probe intensity is determined by the photon number $N=\langle\hat{a}^\dagger\hat{a}\rangle+\frac{1}{2}$ to which we normalize here. The parameter λ takes into account a Lorentzian broadening of the laser beam. The square and curly brackets denote commutator and anti-commutator, respectively. The first term in Eq. (7) does not contribute to the differential absorption because the trace is taken over the steady-state distribution function f_{ij} determined by Eq. (3) resulting in $\mathrm{Tr}\,f=0$. Hence, we focus on the second term. It describes the self-interaction of the electric field mediated by the graphene and therefore contains the pseudospin response function $\theta(t-t')\langle[\hat{\sigma}_x(t),\hat{\sigma}_x(t')]\rangle$ which is sensitive to the presence of coherence. Therefore it adds a signature of the quantum state of the graphene to the outgoing electric field. The steady-state approximation is realized as $\langle[\hat{\sigma}_x(t),\hat{\sigma}_x(t')]\rangle\to\langle[\hat{\sigma}_x(t-t'),\hat{\sigma}_x(0)]\rangle$. The pseudospin is considered in the eigen state basis of $\hat{H}_0$ and its dynamics is governed by the equation $d_t\hat{\sigma}_i(t)=\frac{i}{\hbar}[\hat{H}_0,\hat{\sigma}_i]$. The statistical average is performed as $\langle\sigma_i(t)\rangle=\mathrm{Tr}\,\hat{\sigma}_i(t)f$. In particular, $\langle\sigma_x\rangle=(f_{11}-f_{22})\cos\phi-2\sin\phi\,\mathrm{Im}f_{12}$, $\langle\sigma_y\rangle=(f_{11}-f_{22})\sin\phi+2\cos\phi\,\mathrm{Im}f_{12}$, and $\langle\sigma_z\rangle=2\mathrm{Re}f_{12}$. The resulting correlator reads

$$\langle\mathcal{E}'(0)\mathcal{E}'(0)\rangle_w=\frac{\eta^2_{\omega'}}{\hbar^2}\int\limits_{-\infty}^{0}dt\int\limits_{-\infty}^{t}dt'\sin(\omega' t)\cos(\omega' t')$$
$$\times 4\mathrm{e}^{\lambda t}\mathrm{e}^{\lambda t'}\left[\langle\sigma_y\rangle\sin\phi\sin(\Omega(t-t'))\right.$$
$$\left.+\langle\sigma_z\rangle\cos\phi\sin\phi(\cos(\Omega(t-t'))-1)\right]. \qquad (8)$$

We divide the correlator by the laser pulse duration $\frac{1}{\lambda}$. Then, we employ the rotating wave approximation when

integrating Eq. (8). The result for small $\lambda \ll \omega, \omega'$ reads

$$\langle \mathcal{E}'(0)\mathcal{E}'(0)\rangle_w = -\pi \frac{\eta_{\omega'}^2}{2\hbar^2}\langle\sigma_y\rangle \sin\phi \sum_{\pm} \delta(\omega' \pm \Omega) + \frac{\eta_{\omega'}^2}{\hbar^2}\langle\sigma_z\rangle \frac{\cos\phi \sin\phi\, \Omega^2}{\omega'(\omega'^2 - \Omega^2)}, \tag{9}$$

cf. Eq. (6). In the simplest case of a zero-temperature equilibrium state, we have $f_{22} = 1$, $f_{11} = f_{12} = f_{21} = 0$, hence, $\langle\sigma_y\rangle^{\rm eq} = -\sin\phi$, $\langle\sigma_z\rangle^{\rm eq} = 0$. To calculate the total absorbed energy per unit time and unit area from Eq. (9) we integrate over all momenta and multiply by $\hbar\omega'$. To obtain the relative absorption we divide the result by the incident intensity I_0' and multiply by 4 for the valley and spin degeneracy. The equilibrium absorption then reads

$$A_0 = \frac{\hbar\omega'}{I_0'} 4 \int \frac{{\rm d}^2 k}{4\pi^2} \langle \mathcal{E}'(0)\mathcal{E}'(0)\rangle_w^{\rm eq} = \frac{\pi e^2}{\hbar c}, \tag{10}$$

which is a known result[22]. Most saliently, either of Eqs. (9) and (6) contains non-equilibrium quantum information encoded in the coherences f_{12} and f_{21} whose manifestation can also be seen in the absorption.

Discussion. — We focus on the relative absorption difference $(A - A_0)/A_0$ at $\lambda = 0$ and $\omega \neq \omega'$. This difference is negative due to the so-called Pauli bleaching and reads

$$\frac{A - A_0}{\Gamma\, A_0} = -\frac{\omega'\tau^2}{\omega'^2 - \omega^2}\left(\frac{\omega'^3}{1+\tau^2\omega'^2} - \frac{\omega^3}{1+\tau^2\omega^2}\right) - \frac{2\omega'\tau}{\pi}\frac{\omega'^2 \ln(\tau\omega') - \omega^2\ln(\tau\omega) + \tau^2\omega'^2\omega^2\ln(\omega'/\omega)}{(1+\tau^2\omega^2)(1+\tau^2\omega'^2)(\omega^2 - \omega'^2)}, \tag{11}$$

where $A_0 = \pi e^2/(\hbar c)$ is the equilibrium absorption, and

$$\Gamma = \frac{1}{A_0 I_0'}\frac{\eta_{\omega'}^2 \eta_\omega^2}{\hbar^3 v^2} \tag{12}$$

is a constant that controls the overall signal strength via the coupling parameters η_ω, $\eta_{\omega'}$. We estimate Γ to be of the order of 10^{-5} for typical CW lasers with the power of about 1 mW focused on a μm-size spot and the frequencies ω, ω' being of the order of 0.1 and 1 eV respectively. Measuring such a low signal is a challenging task, however, the relative differential transmission of the order of 10^{-4} has already been measured recently on graphene using an optical pump-probe setup[20]. Note that Γ can be changed in a very broad range by playing with η_ω and $\eta_{\omega'}$, as there is no theoretical limit for excitation frequencies from below (no band gap).

Eq. (11) is among the main results of our work. This signal is a response to the pseudospin superposition states created by η_ω and measured by $\eta_{\omega'}$. The signal should vanish if such states were not there. The relative absorption (11) is solely due to the pseudospin coherence because the conventional occupation-related dip shrinks to zero at $\lambda = 0$. For this reason Eq. (11) does not depend on τ_0 and vanishes at $\tau \to 0$ (very fast dephasing). On the other hand, the signal saturates at $\tau \to \infty$ and equals to

$$\frac{A - A_0}{A_0} = -\Gamma \frac{\omega'}{\omega + \omega'}. \tag{13}$$

The value of the dephasing time τ is unknown but it enters Eq. (11) only in products with ω and ω' resulting in the universal behavior shown in Fig. 2. One can see that reducing ω' affects the signal in the same way as faster dephasing does. On the other hand, faster dephasing is equivalent to higher ω. This effect can also be seen in Eq. (13) vanishing at $\omega \to \infty$ even though dephasing is absent there.

Eq. (11) can be further simplified at $\omega' \gg \omega$ as

$$\frac{A - A_0}{A_0} = -\Gamma \frac{(\tau\omega')^2}{1 + (\tau\omega')^2}\left[1 - \frac{2\ln(\tau\omega')}{\pi\tau\omega'}\right]. \tag{14}$$

As it is expected from Eq. (13), the signal (14) saturates at $\omega'\tau \to \infty$ as $(A - A_0)/A_0 = -\Gamma$. Let us remind that in order to keep $\eta_{\omega'}$ constant in the formal limit $\omega'\tau \to \infty$ we should increase I_0' to infinity as well making this regime experimentally irrelevant. The regime $\omega' \gg \omega$ is most convenient for the pseudospin coherence observation, where the differential absorption is approaching its maximum and, most importantly, the conventional occupation dip at $\omega' = \omega$ is not present even if it is broadened by relaxation.

Conclusion and Outlook. — To conclude, we have demonstrated an analytical framework for a weak measurement description, where the quantum mechanical coherence and carrier statistics are treated using the Liouville-von Neumann equation and, alternatively, the field-field correlator. We apply this approach to intrinsic graphene whose peculiar band structure makes it possible to generate and observe the quantum mechanical pseudospin coherence. The weak measurement of pseudospin coherence is provided by coupling the pseudospin to the electric field of an electromagnetic wave. This coupling is what makes graphene special and, in combination with the results presented above, provides a reliable solid-state platform for fundamental quantum research.

Acknowledgements. — We thank Daniele Brida for multiple discussions of these results. This work was supported financially by the Center of Applied Photonics, an ERC Advanced Grant UltraPhase of Alfred Leitenstorfer and the DFG through SFB 767.

[1] A. Messiah, *Quantum Mechanics* (Dover Publications, 2014).

[2] Y. Aharonov, D. Z. Albert, and L. Vaidman, Phys. Rev.

Lett. **60**, 1351 (1988).
[3] B. Tamir and E. Cohen, Quanta **2** (2013).
[4] K. Resch, J. Lundeen, and A. Steinberg, Physics Letters A **324**, 125 (2004).
[5] G. J. Pryde, J. L. O'Brien, A. G. White, T. C. Ralph, and H. M. Wiseman, Phys. Rev. Lett. **94**, 220405 (2005).
[6] S. Kocsis, B. Braverman, S. Ravets, M. J. Stevens, R. P. Mirin, L. K. Shalm, and A. M. Steinberg, Science **332**, 1170 (2011).
[7] J. B. Götte and M. R. Dennis, New Journal of Physics **14**, 073016 (2012).
[8] L. A. Rozema, A. Darabi, D. H. Mahler, A. Hayat, Y. Soudagar, and A. M. Steinberg, Phys. Rev. Lett. **109**, 100404 (2012).
[9] G.-Q. Liu, J. Xing, W.-L. Ma, C.-H. Li, P. Wang, H. C. Po, R.-B. Liu, and X.-Y. Pan, arXiv:1612.07944.
[10] J. T. Muhonen, J. P. Dehollain, A. Laucht, S. Simmons, R. Kalra, F. E. Hudson, D. N. Jamieson, J. C. McCallum, K. M. Itoh, A. S. Dzurak, and A. Morello, arXiv:1702.07991.
[11] Y. Aharonov, D. Z. Albert, and L. Vaidman, Phys. Rev. Lett. **60**, 1351 (1988).
[12] W. Mao, D. V. Averin, R. Ruskov, and A. N. Korotkov, Phys. Rev. Lett. **93**, 056803 (2004).
[13] A. A. Clerk, M. H. Devoret, S. M. Girvin, F. Marquardt, and R. J. Schoelkopf, Rev. Mod. Phys. **82**, 1155 (2010).
[14] K. Y. Bliokh, A. Y. Bekshaev, A. G. Kofman, and F. Nori, New Journal of Physics **15**, 073022 (2013).
[15] C. Ferrie and J. Combes, Phys. Rev. Lett. **113**, 120404 (2014).
[16] A. K. Geim and K. S. Novoselov, Nat. Mat. **6**, 183 (2007).
[17] M. Trushin and J. Schliemann, New Journal of Physics **14**, 095005 (2012).
[18] F. T. Vasko and A. V. Kuznetsov, *Electronic States and Optical Transitions in Semiconductor Heterstructures* (Springer-Verlag New York, 1999).
[19] Y. Wu and X. Yang, Phys. Rev. Lett. **98**, 013601 (2007).
[20] M. Trushin, A. Grupp, G. Soavi, A. Budweg, D. De Fazio, U. Sassi, A. Lombardo, A. C. Ferrari, W. Belzig, A. Leitenstorfer, and D. Brida, Phys. Rev. B **92**, 165429 (2015).
[21] A. Bednorz, C. Bruder, B. Reulet, and W. Belzig, Phys. Rev. Lett. **110**, 250404 (2013).
[22] R. R. Nair, P. Blake, A. N. Grigorenko, K. S. Novoselov, T. J. Booth, T. Stauber, N. M. R. Peres, and A. K. Geim, Science **320**, 1308 (2008).